

# Spectral imaging using single-axis spectrally dispersed illumination

Yair Bar-Ilan and Dvir Yelin\*

Faculty of Biomedical Engineering, Technion—Israel Institute of Technology, Haifa 3200003, Israel

\*Corresponding author: yelin@tx.technion.ac.il

Received April 9, 2014; accepted July 15, 2014;

posted July 30, 2014 (Doc. ID 209893); published August 27, 2014

Spectral imaging is a powerful tool for a wide variety of applications; however, low imaging rates and signal-to-noise ratios (SNRs) often limit its use for many biomedical applications. Here, we present a technique for spectral imaging using a unique two-dimensional illumination pattern having spectral dispersion in one axis. The method, which is called spectrally dispersed illumination spectral imaging (SDISI), allows high-speed, high-resolution acquisition of spectral data from specimens that often cannot tolerate high illumination intensities or require fast imaging for avoiding motion artifacts. The technique is demonstrated by capturing spectral data cubes of the finger of a human volunteer using short exposure durations and a high (33.5 dB) SNR. © 2014 Optical Society of America

OCIS codes: (170.3880) Medical and biological imaging; (170.6510) Spectroscopy, tissue diagnostics; (110.4234) Multispectral and hyperspectral imaging.

<http://dx.doi.org/10.1364/OL.39.005177>

Measuring the spectrum emitted from each point on a specimen could provide useful information on its chemical and structural composition. The main challenge of spectral imaging, however, is the acquisition, in a timely manner, of the large three-dimensional data sets that may comprise high-resolution spectra within high-pixel-count images. A variety of techniques has been proposed for effective spectral imaging [1], including widefield imaging under different wavelength illumination [2–5], point and line [6] scanning, and full-frame interferometric Fourier spectroscopy [7,8]. Currently, most of the leading manufacturers of optical microscopes offer at least one of these modalities for spectral imaging. In a previous work [9], we demonstrated the feasibility of spectrally encoded endoscopy [10] for capturing spatially resolved spectra by using two-dimensional (2D) scanning of a spectral line across a specimen, while backscattered light was transmitted through an optical fiber and analyzed by a fast spectrometer. This method had a superior signal-to-noise ratio (SNR) compared to point and line scanning [6] and could potentially be useful for various clinical endoscopic applications.

The recent advance in light source technology provided scientists and engineers with a range of high-brightness ultra-broadband light sources; examples of these technologies include supercontinuum light generation in fibers [11] and in vacuums [12]. For many applications, however, there are strict limits to the irradiance levels that a given sample could tolerate. In most biomedical applications, for example, a maximum permissible exposure (MPE) level exists for every tissue type, above which the excitation light would alter the properties of the specimen or induce irreversible damage.

In this Letter, we demonstrate a method for efficient, high-SNR spectral imaging using widefield spatially dispersed illumination. By using a diffraction grating, an off-the-shelf monochromatic camera, and single-axis scanning, we present a method called spectrally dispersed illumination spectral imaging (SDISI), analyze the system's optical performance, and demonstrate high-SNR imaging of the finger of a human volunteer.

The optical configuration of the SDISI system, schematically illustrated in Fig. 1(a), is essentially a 2D widefield variant of the recently published spectrally encoded spectral imaging (SESI) technique [9]. By illuminating a large area and detecting spectrally encoded reflectance from an entire sample plane, spectral imaging is efficiently conducted at low irradiance levels and without the need for rapid 2D scanning. A spatially coherent light beam from a broadband supercontinuum source (SC-400, Fianium Ltd.) was low-pass filtered to remove wavelengths above 800 nm, magnified ( $\times 4$ ) using two achromatic lenses,

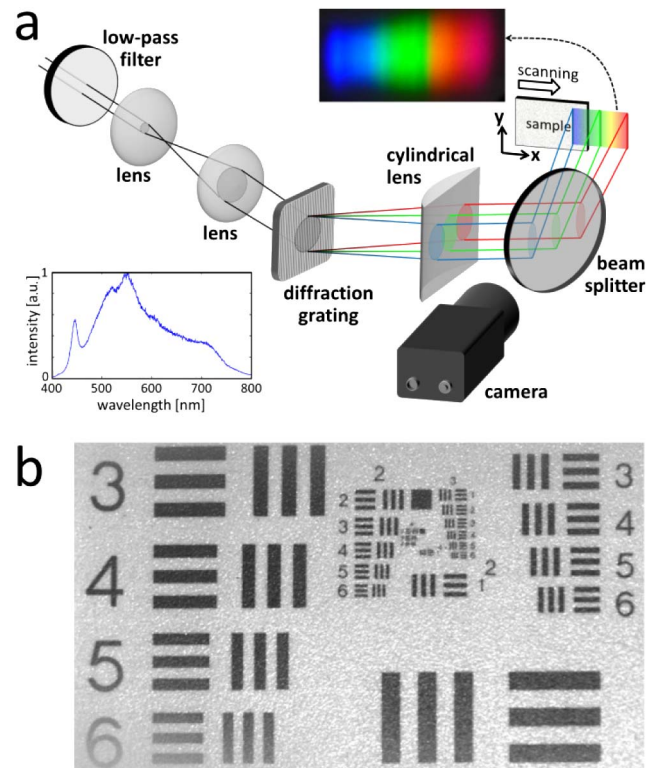


Fig. 1. (a) Optical setup of SDISI. Top inset: color photograph of the illumination pattern. Bottom left inset: illumination spectrum. (b) Monochrome image of a black-on-white scattering resolution target.

diffracted by a 600 line/mm transmission grating, focused in the horizontal axis ( $x$ ) by a cylindrical lens (75 mm focal length), and deflected toward the sample using a 50:50 50-mm-diameter beam splitter. The resulting spectrally dispersed illumination pattern [Fig. 1(a), top inset] covered a  $24.8 \times 10.3$  mm rectangle spanned by the diffraction grating and by the cylindrical lens in the horizontal ( $x$ ) and vertical ( $y$ ) axes, respectively. The light reflected from the sample was imaged through the beam splitter using a multielement lens (25 mm focal length,  $f$ -number = 4) and a high-resolution monochrome camera (5 M pixels, 15 frames/s, Sony XCL-5005). An exemplary reflectance image of a scattering resolution target (black ink on a white background), normalized to the illumination pattern intensity, is shown in Fig. 1(b), demonstrating lateral resolution of approximately  $17 \mu\text{m}$  and a field of view of 16.5 and 10.3 mm in the  $x$  and  $y$  axes, respectively.

Spectral data acquisition was conducted by repeatedly capturing images at the maximum frame rate of the camera (15 Hz) while the sample was slowly translated along the spectral  $x$  axis using a motorized linear translation stage. Once a full scan was completed, a spatial-spectral data cube was assembled by digitally stacking the camera images with a small shift ( $d$ ) that corresponded to the distance that the sample had moved between subsequent frames. The formation of the spatial-spectral cube is schematically illustrated in Fig. 2, depicting the gradual transition of two exemplary red and green features across the illumination spectral pattern. As each sample location passed through different illumination wavelengths, its reflectance was varied according to its own reflection spectrum, resulting in a gradual capture of the full spectrum from each resolvable sample location.

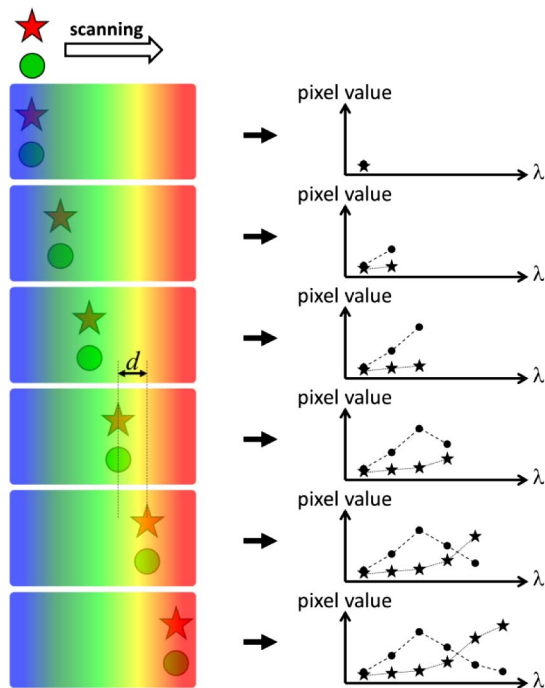


Fig. 2. Acquiring spectra using SDISI. A sample comprising a red star and a green circle is scanned across the spectrally dispersed illumination, resulting in the gradual capture of the reflection spectrum from each sample location. Star (circle) markers correspond to the reflection intensity from the red star (green circle).

In order to measure the spectral accuracy of the system, we have imaged a calibration color card (X-Rite Inc.) and compared the resulting spatially averaged spectra from each colored square [Fig. 3(a), blue curves] to the spectra measured by a commercially available spectrometer (USB2000+, Ocean Optics Inc., red curves). A good agreement between the spectra was evident within the 450–700 nm wavelength range. The ability of the system to measure true color was assessed by transforming the measured spectra into apparent colors [13]. Due to the lack of blue wavelengths below 450 nm in the illumination spectrum, a strong color bias toward red hues was evident in all measured colors [Fig. 3(b)]. A digital photograph of the target is shown for reference in Fig. 3(c).

In order to demonstrate spectral imaging of live tissue, the finger of a human volunteer was scanned in the  $x$  axis at a velocity of 0.6 mm/s and imaged at a rate of 15 frames/s. The raw data set comprised 1100 overlapping images that resulted in 600 individual wavelengths measured for each sample location (approximately 0.5 nm wavelength sampling intervals). The total illumination power was 250 mW, resulting in an average irradiance of approximately  $78 \text{ mW/cm}^2$  on the finger. The exposure duration of each frame was only 0.1 ms, and the total imaging duration was 73 s; both were limited by the camera electronics. Individual spectra of selected locations from the effective  $750 \times 1800 \times 600$  pixel data cube (the  $x$ ,  $y$ , and  $\lambda$  axes, respectively) are shown in Fig. 4, indicated on a single selected frame of the finger. Some of the spectra (refer to the top right spectrum in Fig. 4, for example) within the data cube clearly showed the distinctive spectral pattern of oxyhemoglobin that is characterized by two reflection dips at 545 and 570 nm [14].

For deriving the SNR of SDISI, we follow the general notation in [9]. The maximum signal (in electrons) measured for each resolvable element ( $x$ ,  $y$ ,  $\lambda$ ) is given by  $Q_e r [I_{\text{max}} s / (h\nu)] t$ , where  $Q_e$  denotes the detector quantum efficiency,  $r$  denotes sample reflectivity,  $I_{\text{max}}$  denotes the MPE in units of  $\text{W/cm}^2$ ,  $s$  denotes the area of a single

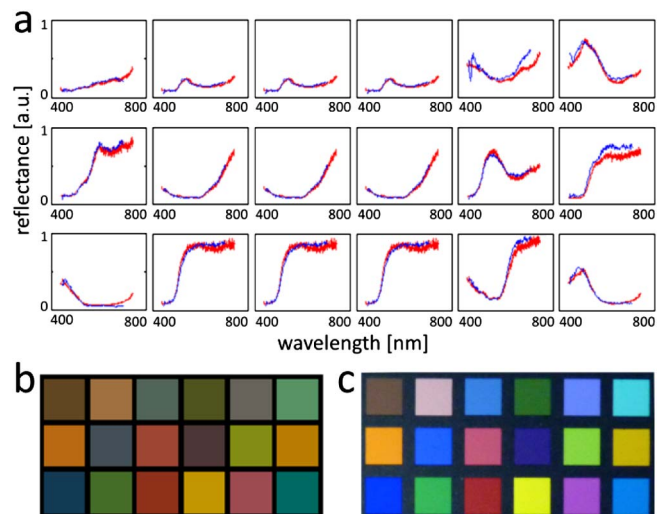


Fig. 3. (a) Averaged SDISI spectra (blue curves) of a color calibration target compared to spectra measured by a commercial spectrometer (red curves). (b) Corresponding colors of the SDISI curved spectra in (a) show lack of blue hues. (c) A color photograph of the target.

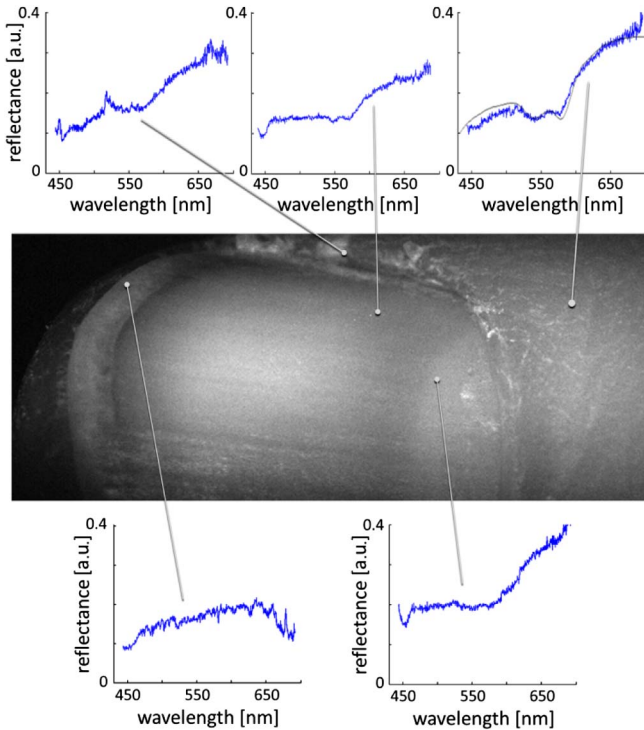


Fig. 4. Selected reflectance spectra (blue curves) from SDISI of a volunteer's finger. Spectrum of oxyhemoglobin (gray curve) is shown in the top right plot for reference.

spatial resolvable element,  $h$  is the Planck constant,  $\nu$  denotes the optical frequency, and  $t$  denotes the exposure time for a single resolvable element. Because the illumination is spectrally dispersed, each pixel in a single  $N \times N$  pixel (square) frame is transiently illuminated by a single wavelength, while the reflected light from that pixel is detected during an exposure time given by  $t = T/(N + M)$ , where  $T$  denotes the total data acquisition time and  $M$  denotes the number of spectral resolvable elements along the  $x$  axis ( $N, M \gg 1$ ). Assuming that the dark current  $D$  is the dominant noise source (neglecting shot and read noise), the SNR is given by

$$\text{SNR}_{\text{SDISI}} \cong \frac{Q_e r I_{\text{max}} s t}{\sqrt{D} t} = \frac{Q_e r I_{\text{max}} s \sqrt{T}}{h \nu \sqrt{D}} \sqrt{\frac{1}{N + M}}. \quad (1)$$

Assuming for brevity that  $M = N$ , the SNR in Eq. (1) is  $N^{1/2}$  times higher than the SNR of the previously reported endoscopic SESI technique [9] and  $N/\sqrt{2}$  times higher than spectral imaging using line scanning [6]. In applications that involve high pixel counts, these figures represent significant, several-fold improvement in SNR. In the current SDISI system, however, speckle contrast was relatively high and was equal to approximately 0.1 for a single-point spectrum on the sample. Using spatial averaging over several neighboring pixels helped reduce speckle noise; the average SNR for imaging the human finger (refer to Fig. 4) was approximately 33.5 and 27 dB for the spectral and image data, respectively. These SNRs were achieved using short 0.1 ms exposure durations for each frame, which is equivalent to acquisition rates of up to nine spatial-spectral data cubes per second. Effective video-rate spectral imaging would thus be possible using

higher frame-rate cameras having comparable levels of dark currents (i.e., cooled detector array).

In contrast to most spectral imaging methods, in SDISI, the spatial and spectral resolutions are directly linked; the maximum number of resolvable wavelengths is essentially limited by the number of resolvable points in a single frame. In specific cases where high spectral resolution is not necessary, the user may choose to increase the physical step size between frames, resulting in higher acquisition rates of undersampled spectra. The challenges toward practical implementation of SDISI are related mainly to the generation of the somewhat complex illumination pattern and to the calibration and alignment procedures of the illumination and the imaging optics. Also, in its current form, SDISI would be effective in measuring reflectance, absorption, and backscattering from a specimen but is not suitable for spectral imaging of fluorescence markers due to the inherent difference between their excitation and emission spectra. Also, compared to SESI [9], SDISI would be less suited for endoscopic applications within narrow ducts due to the lack of an encoding technique and reliance on a full 2D image capture.

In summary, we have demonstrated a new method for spectral imaging using spectrally dispersed illumination. The system was analyzed using spectral imaging of resolution and color test targets and demonstrated by imaging the finger of a volunteer using submillisecond frame exposures and high SNRs. Compared to current point-and-line-scanning techniques, SDISI exhibits an orders-of-magnitude advantage in SNR and is capable of high spectral and spatial resolutions.

This study was funded in part by the European Research Council Starting Grant (239986) and by the Israel Science Foundation (716/09). This work was also supported in part by the Lorry I. Lokey Interdisciplinary Center for Life Sciences and Engineering.

## References

1. D. L. Farkas and D. Becker, *Pigment Cell Res.* **14**, 2 (2001).
2. C. L. Wyatt, *Appl. Opt.* **14**, 3086 (1975).
3. R. D. Shonat, E. S. Wachman, W.-H. Niu, A. P. Koretsky, and D. L. Farkas, *Biophys. J.* **73**, 1223 (1997).
4. P. J. Miller, *Metrologia* **28**, 145 (1991).
5. X. Gao, Y. Cui, R. M. Levenson, L. W. K. Chung, and S. Nie, *Nat. Biotechnol.* **22**, 969 (2004).
6. M. B. Sinclair, J. A. Timlin, D. M. Haaland, and M. Werner-Washburne, *Appl. Opt.* **43**, 2079 (2004).
7. Y. Garini, M. Macville, S. du Manoir, R. A. Buckwald, M. Lavi, N. Katzir, D. Wine, I. Bar-Am, E. Scherock, D. Habib, and T. Ried, *Bioimaging* **4**, 65 (1996).
8. Z. Malik, D. Cabib, R. A. Buckwald, A. Talmi, Y. Garini, and S. G. Lipson, *J. Microsc.* **182**, 133 (1996).
9. A. Abramov, L. Minai, and D. Yelin, *Opt. Express* **19**, 6913 (2011).
10. D. Yelin, I. Rizvi, W. M. White, J. T. Motz, T. Hasan, B. E. Bouma, and G. J. Tearney, *Nature* **443**, 765 (2006).
11. J. M. Dudley, G. R. Genty, and S. P. Coen, *Rev. Mod. Phys.* **78**, 1135 (2006).
12. S. Horne, D. Smith, M. Besen, M. Parlow, D. Stolyarov, H. Zhu, and W. Holber, *Proc. SPIE* **7680**, 76800L (2010).
13. G. Engel, H. Genish, M. Rosenbluh, and D. Yelin, *Biomed. Opt. Express* **3**, 1855 (2012).
14. W. G. Zijlstra, A. Buursma, and W. P. Meeuwse-van der Roest, *Clin. Chem.* **37**, 1633 (1991).